

Design and Implementation of a Control System for the
Mesabi V27 Wind Turbine

A THESIS
SUBMITTED TO THE FACULTY OF THE GRADUATE SCHOOL
OF THE UNIVERSITY OF MINNESOTA
BY

William M Thorson

IN PARTIAL FULFILLMENT OF THE REQUIREMENTS
FOR THE DEGREE OF
MASTER OF SCIENCE

Peter J. Seiler, advisor

May 2013

Acknowledgments

There are many people that have earned my gratitude for their contribution to my time in graduate school. These include Professors Peter Seiler, Gary Balas and Ned Mohan for serving on the Master's Committee, and for advising my design process. Caleb Carlson deserves special thanks for development of the yaw control system presented herein. Matt Leuker is also worthy of many thanks for his assistance in the programming of the cRIO and advising the hardware purchases. And finally, all of my gratitude goes to Instructor Dan Janisch, John Liimatta, and the other students in the wind program at the Mesabi Range Community and Technical College for making this project possible, with their many hours of work on hardware for this turbine.

Abstract

The focus of this thesis is the design and implementation of a control law for a Vestas V27 turbine. There are two motivations for this work. First, there is a rapidly growing industry to refurbish turbines and the proposed control design can be used to update V27 turbines to extend their operational life. Second, the proposed control design will be open-source thus enabling the V27 turbine to be used for research purposes. The thesis will first provide a review of traditional wind turbine control systems. Next the V27 turbine hardware, software, and design specification are described. A control system is then described that includes supervisory control and a SISO classical control for the rotor speed tracking controller. Experimental test results are presented using a V27 turbine installed at the Mesabi Range Community and Technical College.

Contents

List of Tables	vi
List of Figures	vii
Chapter 1 Introduction	1
1.1 Wind Turbine Basics	1
1.2 Turbine Control	4
1.2.1 Turbine Modeling	4
1.2.2 Turbine Operating Regions	6
1.2.3 Region 2 Control	7
1.2.4 Region 3 Control	10
1.3 Turbine Power Electronics	10
Chapter 2 Vestas V27 and Turbine Controls	12
2.1 V27 Situation and Future Research	12
2.2 V27 Operation and Specifications	14
2.3 Subsystems	17
2.3.1 Blade Pitch System	17
2.3.2 Rotor Speed Measurement	17

2.3.3	Yaw System	19
2.3.4	Anemometer and Wind Vane	20
2.4	Hardware and Software	21
2.4.1	Matlab for Control Design, Simulation and Development	21
2.4.2	Control Hardware	22
2.4.3	Control Software Implementation	23
2.5	Other Control Goals	24
Chapter 3 Control Design		25
3.1	Programming and Testing Interface	25
3.2	Supervisory Control	27
3.2.1	State: Emergency	27
3.2.2	State: Stop	29
3.2.3	State: Pause	29
3.2.4	State: Run	30
3.3	Blade Pitch Control	31
3.3.1	Blade Pitch Subsystem	31
3.3.2	Pitch Controller Inputs and Outputs	32
3.3.3	Blade Pitch and Rotor Speed Tracking	33
3.4	Yaw Controller	35
Chapter 4 Testing and Results		36
4.1	Rotor Speed Tracking	36
4.2	Modeling the Blade Pitch Actuator	37

4.3	Blade Pitch Tracking	40
4.4	Modeling the Turbine Rotor	41
Chapter 5	Conclusions and Future Work	46
	Bibliography	48
	Appendix A Photos of Turbine Hardware	50
	Appendix B Physical Parameters of the V27 Wind Turbine	52

List of Tables

2.1	Generator specifications provided for V27 at 50 Hz [1].	16
B.1	General specifications for V27 [1].	53

List of Figures

1.1	Illustration of a typical wind turbine setup. US DOE	2
1.2	The Clipper C96 EOLOS research turbine in Rosemount, MN [2].	3
1.3	The C_p curve for the CART3 wind turbine at NREL [3].	5
1.4	The incident-wake interaction of wind in the turbine blades [4].	6
1.5	The 4 regions of control for wind turbine operation [2].	7
1.6	The Standard Control Law shown in a feedback diagram.	9
1.7	The C_p versus TSR curve for the CART3 [3].	9
2.1	The Vestas V27 in Eveleth, MN	13
2.2	Left to right: EOLOS C96, NREL CART3, MRCTC V27	15
2.3	Estimating the rotor speed from the measurement signal.	19
2.4	The anemometer and wind vane on the turbine nacelle.	20
3.1	A simplification of the control architecture implemented in Simulink.	26
3.2	The testing interface, showing VeriStand and the V27.	26
3.3	Supervisory controller structure as implemented in Stateflow.	28
3.4	The blade pitch command state subsystem.	32
3.5	Closed-loop blade pitch system.	33
3.6	The full blade pitch subsystem.	34

4.1	Closed-loop rotor speed controller without blade pitch sensor.	37
4.2	Step command of desired rotor speed, no blade pitch inner-loop.	38
4.3	The cRIO in the nacelle, and pitch actuator amplifier.	39
4.4	Characterizing the blade pitch actuator.	40
4.5	First step for blade pitch reference tracking.	41
4.6	Second step for blade pitch reference tracking.	42
4.7	Rotor speed response for a step change in blade pitch. Test 1.	43
4.8	Rotor speed response for a step change in blade pitch. Test 2.	44
4.9	Rotor speed response for a step change in blade pitch. Test 3.	45
A.1	The cRIO in the tower base used for CBM.	51
A.2	The hydraulic motor in the nacelle.	51

Nomenclature

Abbreviations and Acronyms

<i>MRCTC</i>	Mesabi Range Community & Technical College
<i>HAWTs</i>	Horizontal Axis Wind Turbines
<i>ISO</i>	Independent Systems Operator
<i>TSR</i>	Tip Speed Ratio
<i>cRIO</i>	Compact Reconfigurable Input/Output
<i>SISO</i>	Single-Input, Single-Output
<i>MIMO</i>	Multi-Input, Multi-Output

List of Symbols

λ	Tip Speed Ratio, TSR
ω_{rot}	Rotor Rotational Velocity , <i>rads/sec</i>
C_p	Coefficient of Power
R	Rotor Radius, <i>meters</i>
V_∞	Free-stream/Upwind Wind Velocity, <i>m/s</i>
V_{rotor}	Velocity of Wind Incident to the Rotor, <i>m/s</i>
V_d	Down-wind Wind Velocity, <i>m/s</i>

Chapter 1

Introduction

Presented within this thesis is a design for a controller for a Vestas V27 wind turbine. This turbine is intended to generate power, as well as be used for teaching and research purposes. The design of the controller followed the need to meet these objectives safely and keep the control structure simple and the controllers easily modifiable. Chapter 1 provides a brief introduction into turbine mechanics and control objectives associated with wind turbines. Chapter 2 introduces the reader to the problems and objectives associated with the V27 wind turbine. In Chapter 3 discusses the design process for building the controller for the turbine. Chapter 4 describes the simulation process and test results for the new controller.

1.1 Wind Turbine Basics

Wind turbines are systems that take mechanical energy from the wind and convert it to electrical energy. Many types of wind turbines exist today, with variations in rotation axis, number of blades, control surfaces and generator type being among the most common differences between turbines in the industry. The most prevalent turbines studied in the controls literature are the 3-bladed, upwind, horizontal axis wind turbines (HAWTs). These turbines operate with a vertical plane arrangement of evenly spaced blades and an active yaw system to bring the rotor-blade plane perpendicular to the prominent wind direction. HAWTs are studied often primarily because of their dominance in the marketplace and their use of active controls [5].

Wind turbines have become increasingly prevalent on the electric grid, and constitute

one of the largest new sources of grid capacity in the United States in recent years. In 2011, wind power comprised 32% of added grid capacity in the United States and 42 GW of wind power capacity was added world wide. Wind power has seen a cumulative investment of \$95 billion since the beginning of the 1980s in the U.S. Wind is estimated to account for 3.3% of the supply of electricity generated in the U.S., and sees penetrations as high as 29% in Denmark. Along with this increase in prevalence, utility scale wind turbines are getting larger. The average hub height has increased by 45% and the average rotor diameter has increased by 86% since 1998, and further increases are expected [6].

With this increase in the prevalence of wind turbines, turbine control systems are becoming more important. Regional Independent Systems Operators (ISOs) are requiring more control over turbine functionality. ISOs require wind turbines to be an active part of keeping the quality and availability of electricity high. Maintaining grid voltage and frequency while reducing harmonics in current are objectives that require participation from all generators. Up until this point, wind turbines and farms were considered a negative load, and the rest of the system was responsible for following this highly variable resource. As turbines become a more vital part of the energy market, classifying them as a negative load and allowing the injection of any power is not feasible for sustaining grid quality [7].

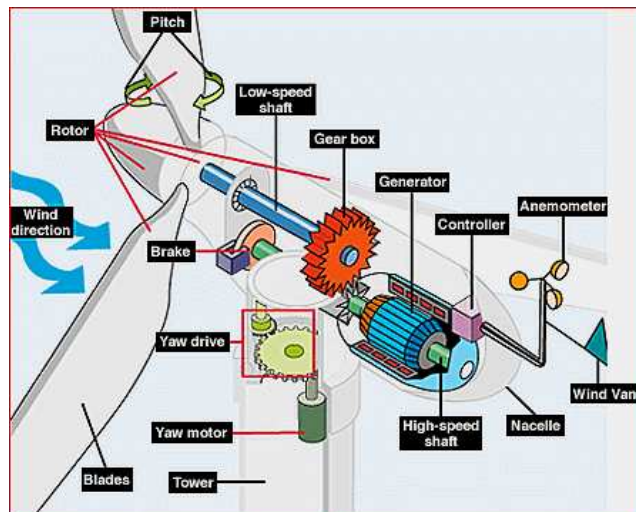


Figure 1.1: Illustration of a typical wind turbine setup. US DOE

Figure 1.1 shows a diagram of a typical horizontal axis wind turbine. The wind comes

in perpendicular to the direction of the rotor plane, a direction which is actively controlled by the turbine yaw drive. The blades are allowed to pitch along their main axis, controlling the amount of lift that is generated from the wind. The torque created by the lift is transported down the low-speed shaft, then through a gearbox. The gearbox transforms the low rotational frequency to something high enough for optimal electrical generation in the generator. The nacelle sits at the top of the tower and provides the connection point to the rotor, as well as housing the generator, gearbox, and controller for the wind turbine. The anemometer and wind vane work together to provide wind speed and wind direction for the turbine controller.

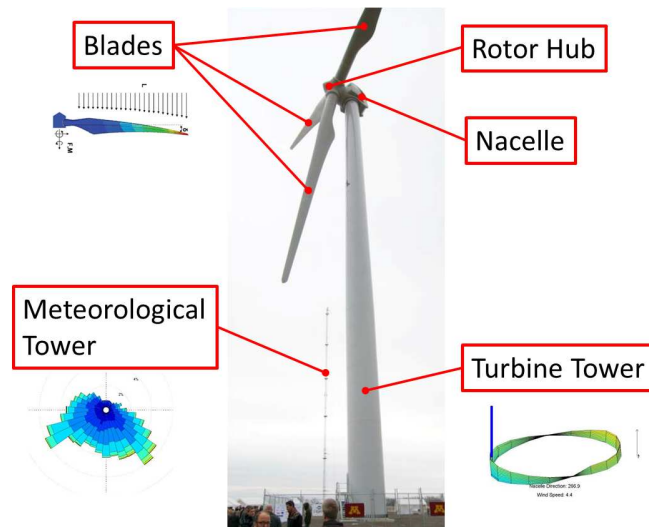


Figure 1.2: The Clipper C96 EOLoS research turbine in Rosemount, MN [2].

Figure 1.2 shows the EOLoS wind turbine used by researchers at the University of Minnesota in partnership with the U.S. Department of Energy. It is a Clipper C96, 2.5MW wind turbine located in Rosemount, MN. The turbine is set up for research purposes, with measurement devices for structural health monitoring already set up. The turbine will soon be equipped with a processor that can be used for implementing control laws designed by University researchers. The meteorological tower provides data for conditions in the immediate area that are very useful for model verification and controls.

1.2 Turbine Control

1.2.1 Turbine Modeling

The power available from the wind is given by

$$P_{wind} = \frac{1}{2}\rho Av_{wind}^3 \quad (1.1)$$

where ρ is the local air density, A is the swept area of the turbine blades, and v_{wind} is the wind speed incident to the rotor [8, 9]. The power captured by the turbine blades is proportional to a factor known as the coefficient of power. The coefficient of power, given as $C_p(\beta, \lambda)$, is a measure of the efficiency of power captured by the wind turbine.

$$C_p(\beta, \lambda) := \frac{P_{captured}}{P_{wind}} \quad (1.2)$$

λ , known as the Tip Speed Ratio (TSR), is a ratio of the blade tip speed, $\omega \times R$, to the incident wind speed. The TSR has been found to be a useful metric when tracking the maximum power point, $C_{p,max}$.

$$\lambda = \frac{\omega R}{v_{wind}} \quad (1.3)$$

The coefficient of power is determined from flow simulations and field testing of the turbines, and used to provide a more clear model of the steady-state turbine system. Figure 1.3 shows a typical C_p curve for a turbine. Calculations of the efficiency are based on static aerodynamic analysis. Therefore the given C_p is expected to be more accurate in steady-state and less accurate in dynamic wind conditions. Discrepancies appear when analyzing raw data, and it would be useful to have a model that more accurately determined efficiency in dynamic conditions.

The power coefficient is a highly variable measure in fielded turbines. Several factors actually alter this value from the OEM specifications. These include the location of the turbine and slight variations in the production of components. C_p can change over time for a single turbine due to structural wear. Research is currently taking place accounting for this variability and considering methods for either tracking maximum

C_p as a time-dependent variable or tracking maximum power without considering the coefficient explicitly [3, 10].

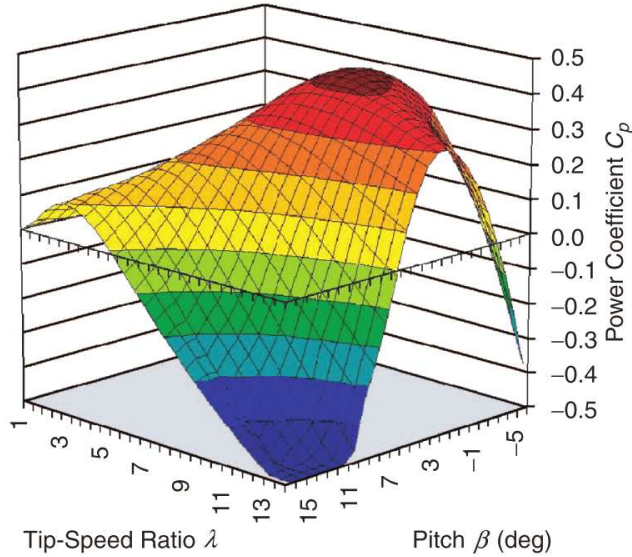


Figure 1.3: The C_p curve for the CART3 wind turbine at NREL [3].

The primary aim of control is to maximize amount of available power that is captured by the turbine. This goal is bounded by a fundamental constraint known as Betz Law. The limit follows from the fluidity of the wind, and the nature of incompressible flow. Wind that is in an unperturbed steady state is characterized by a free stream velocity, V_∞ . As the wind passes through the turbine blades, V_{rotor} , the momentum that it carries is captured as energy by the blades. With less energy, the wind then slows down to a new steady state velocity, V_d , and spreads out in the wake of the turbine rotor (Figure 1.4). Due to incompressible flow, the wind speed can only slow a finite amount. The result is that the power extracted is limited to $16/27^{th}$ s of the power available in the wind [8, 9]. This value is known as the Betz limit. Current wind turbines have not reached this Betz limit in operational efficiency, and much of the strive in the academic fields is to find a way to close this gap [3].

The power extracted from the wind accelerates the turbine blades to the operating speed. A one-state model for the wind turbine dynamics is often presented in order to aid in the design of power controllers. The torque generated by the aerodynamic interaction of the blades and the wind is given by Equation 1.4.

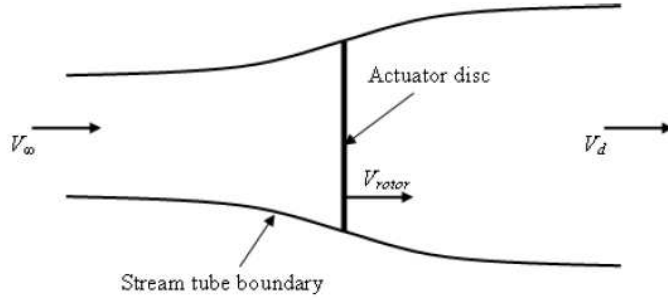


Figure 1.4: The incident-wake interaction of wind in the turbine blades [4].

$$\tau_{capt} = \frac{1}{2} \frac{\rho A v^3 C_p}{\omega} \quad (1.4)$$

In this one-state model, shaft dynamics are ignored, and J_{eq} is the rotor equivalent inertia. The change in rotational velocity is the difference between torque created by capturing wind and generator torque over the inertia, as presented in Equation 1.5.

$$\dot{\omega} = \frac{1}{J_{eq}} (\tau_{capt} - \tau_{gen}) = \frac{1}{J_{eq}} \left(\frac{P_{capt}}{\omega} - \tau_{gen} \right) \quad (1.5)$$

This one-state model is used in control designs for both blade pitch actuators and generator speed control. The result is useful, but it suffers from limitations when ignoring gearbox, blade and tower flex modes. These modes are important when considering loading effects, which is a common concern in current turbine research [7].

1.2.2 Turbine Operating Regions

HAWTs have four operating regions for medium and large scale wind turbines. The region is determined by the average wind speed over the turbine rotor area. An image outlining these four regions is shown in Figure 1.5. The first region is between zero wind and the cut-in wind speed. In this range, the wind speed is below the threshold for effective production of electrical energy. The generator is off and the turbine is left in a neutral state with the blades pitched for reduced capture. The goal in this region is to reduce the chance of unnecessary structural that does not correspond with producing any revenue.

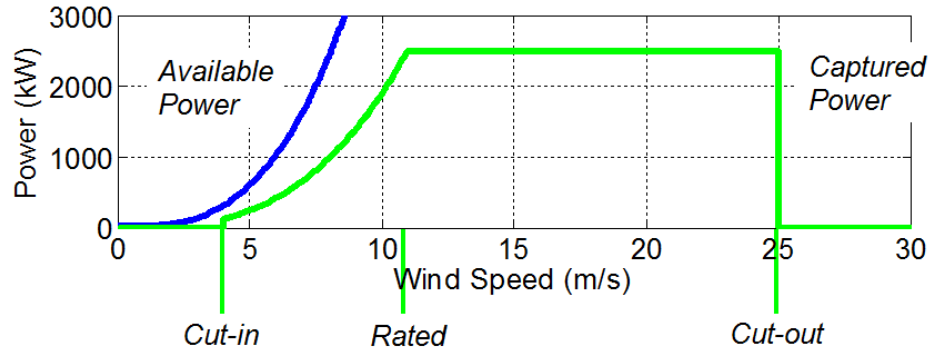


Figure 1.5: The 4 regions of control for wind turbine operation [2].

The second region is between the cut-in and rated wind speeds. This region effectively takes the turbine from zero electrical energy production to rated, nameplate energy production. The control objective is to maximize the energy capture of the turbine. The standard control law, a method for choosing the generator torque in order to maximize the capture efficiency at any given rotor speed, is the most commonly used control effort.

The third region is between the rated wind speed and the cut-off wind speed. Blade pitch control is commonly used to track the optimal rotor speed, leaving the power generated at the rated level. Another control objective in this region is to reduce structural loading on the turbine that may be caused by wind gusts or other turbulence. There is plenty of research being done on region 3 control, as material and maintenance savings present the next major source of cost savings.

Finally, the fourth region is beyond the cut-off wind speed. Above this wind speed, the turbine may face structural damage as turbine components were not designed for the stress that is applied due to the force of the wind. The blades pitched for minimal capture, the generator is disconnected and the turbine is yawed so that the blades are parallel to the flow of the wind [11].

1.2.3 Region 2 Control

In Region 2, the wind speed varies greatly, and therefore the power available to the generator is variable in this region. In induction turbines, the rotor speed is approximately constant for any wind speed where it is intended to produce power.

Normally this would mean operation at the trim pitch position, but it could mean other pitch angles if curtailment is desired. These induction generators are simple, but it allows for limited controls applications. Other turbines, such as permanent magnet generators with a full power electronics interface to the electrical grid, can operate at variable rotor speeds.

There are many benefits to having a greater degree of control over the rotor speed at these lower wind speeds. The turbine may respond better to the strains applied at different rotor speeds depending on, for instance, the turbulence of the wind. There is also an opportunity to dampen vibrational modes existing in the turbine. Although design of the turbine is thorough, there would be substantial advantages in reducing possible loading effects on the turbine, including reducing production costs by using cheaper and lighter materials. With generator control, the power electronics systems and blade pitch control can act simultaneously to mitigate the stresses resultant on the blades or the turbine shaft. Research is being done studying H_∞ methods for reducing this loading on the turbines.

Another reason for generator control in Region 2 is the opportunity to operate at the maximum power coefficient for any given wind condition. A slice of a C_p curve for a fixed blade pitch is shown in Figure 1.7. Of course, the turbine is usually designed with the maximum capture coefficient corresponding to the most likely wind condition and the rated power in mind. The set point for this optimal value would likely be the point where a steady state wind would result in exactly the rated wind speed, with the blades in the trim condition, as this would constitute the minimum energy required in order to achieve this power. But as can be clearly seen from the figure, the efficiency drops quickly from this peak value as the wind speed changes, especially if the rotor speed is not fast enough for the wind condition.

One technique for tracking the optimal Tip Speed Ratio is with the Standard Control Law [3], shown in Figure 1.6. The Standard Control Law uses the rotor rotational speed to calculate a desired torque for the control signal, as shown in Equation 1.6.

$$\tau_{gen,comm} = K\omega^2 \tag{1.6}$$

The control gain, K , is based on the maximum power coefficient, $C_{p,max}$, and the TSR that results in that maximum, λ_* . The desired blade pitch, β_{opt} , is usually the

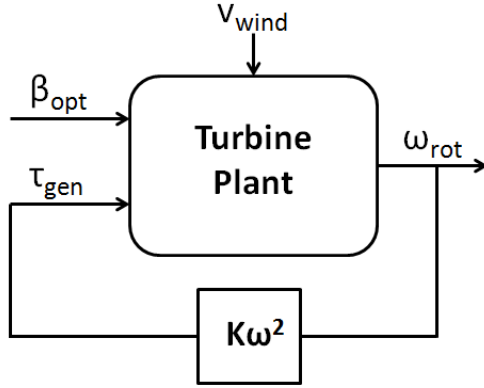


Figure 1.6: The Standard Control Law shown in a feedback diagram.

trim condition, and the wind speed, v_{wind} , is treated as a disturbance. The quadratic, $F(\lambda) = \frac{C_{p,max}}{\lambda_*^3} \lambda^3$, shown in Figure 1.7, tracks the optimal C_p .

$$K = \frac{1}{2} \rho A R^3 \frac{C_{p,max}}{\lambda_*^3} \quad (1.7)$$

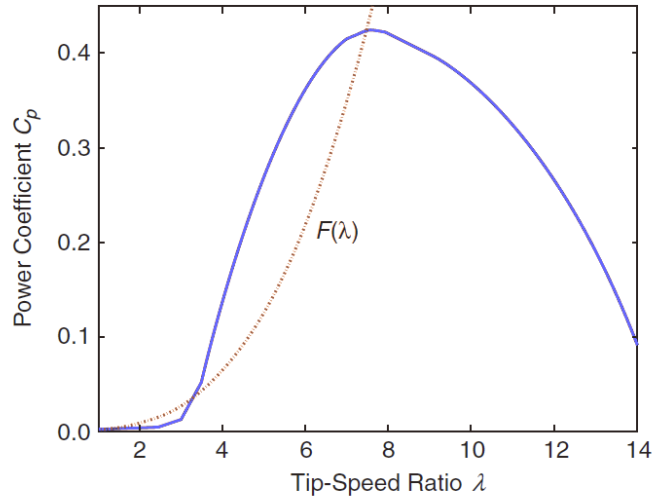


Figure 1.7: The C_p versus TSR curve for the CART3 [3].

This results in the rotor speed converging to the optimal tip speed. There are issues with this approach. As mentioned previously in Section 1.2.1, the C_p curve varies for individual turbines and changes over time. Research is being done on a time-varying

version of this Standard Control Law approach [3].

1.2.4 Region 3 Control

Turbines operating in Region 3 are beyond the rated wind speed, and therefore need only to maintain the desired power rather than seek an optimal generator speed. The control effort no longer tracks only the maximal power output but seeks to mitigate loading effects on the turbine, as described in Section 1.2.3. The bulk of the control effort in Region 3 is by the blade pitch system. Blade pitch actuators are slow relative the frequency of stochastic disturbances in the wind speed, but blade pitch control is useful for average wind speed tracking.

There is research being conducted on multi-input, multi-output approaches to the control effort in Region 3. Generator torque control can be used to respond to the higher frequency fluctuations in the wind speed. This can potentially greatly reduce loading when wind speed is turbulent.

1.3 Turbine Power Electronics

Several types of generators exist, all with their own limits for power control. The induction generator directly coupled to the grid, sometimes referred to as a Type I turbine, is the least controllable of the turbines. The only control that the operator has over the power generated comes from the pitch of the blades. These turbines are asynchronous generators because the output current does not correspond exactly to the generator voltage. The amount of power generated by these turbines is proportional to the difference in the frequency of the rotor high speed shaft, given in electrical radians per second, to the grid frequency [12, 13].

Electrical radians per second are different than rotor radians per second in multi-pole systems, meaning that the current makes $p/2$ times as many cycles per rotation of the rotor, where p is the number of electrical poles in the generator. The difference in the speeds, called the slip, required for maximum power production is generally only 1 to 2 percent of the nominal generator electrical speed. In contrast, the slip can be varied to a rate of 10% in wound rotor induction generators with variable rotor resistance (Type II turbines), and to 50% in doubly fed asynchronous generators (Type III). These are more complicated due to the variable resistance and full power electronics feedback, respectively.

Type I turbines are in contrast to the common Type IV turbines, which are on the other spectrum of control capability. Type IV turbines, like the Clipper C96 research turbine in Rosemount, have a full power electronics decoupling between the turbine generator and the electric grid. This addition allows for the generator torque control that is described in section 1.2.4. The generator is a permanent magnet AC machine and current is produced directly by the magnets changing the flux in the stator coils. Thus, the turbine is a synchronous generator as the rotor magnet passing a stator coil corresponds directly to a current, so the generator electrical frequency on the output side is what would be output on the grid. Because of this, it is easy to see that these turbines will not function without the full power electronics interface, at least not with variable power output, and therefore these turbines have a large extra cost built-in.

The DC to AC conversion associated with the power electronics interfaces makes it possible to control the output reactive power. This is becoming ever more important in the wind industry. Reactive power is the imaginary portion of the absolute power, S . When the output current is out of phase with the output voltage, the result is that some of the power is reactive. Reactive power is necessary to maintain voltage stability on the electric grid; for example, a shortage in reactive power can result in grid collapse if the system is overloaded. Reactive power can be injected or removed from the grid using reactive power compensation, but overuse is costly. For this reason, regional ISOs are beginning to require that wind plants, as other power plants, be able to control the power factor of the plant. The output power electronics do this by changing the timing of the individual diodes' triggering, in turn altering the phase of the output current relative to the grid voltage. This is not possible with induction generators that are not decoupled from the grid.

Chapter 2

Vestas V27 and Turbine Controls

The Vestas V27 turbine offers a unique opportunity for research and education purposes. The turbine requires an entirely new control system, however, as it was originally designed for the European 50 Hz grid. A substantial amount of engineering is necessary when designing this control system.

2.1 V27 Situation and Future Research

The V27, shown in Figure 2.1, is a 225kW turbine produced by Vestas in the 1980s. This turbine was purchased by the Mesabi Range Community and Technical College (MRCTC) and installed on their Eveleth, Minnesota campus. The turbine was purchased to facilitate the Wind Energy Technology Program based at that campus. In this degree program, students learn about basic electronics, wind turbine mechanical and electrical operation, tower safety, turbine maintenance, and other related topics. Having the turbine on the campus gives the students practical experience as it allows them to perform standard tests without travel. More importantly, the turbine is owned by the school, so any climbing of the tower and control is easily approved, something which isn't possible in an industry owned wind turbine. For this reason, it is an invaluable resource to the Mesabi program.

However, the turbine presented many challenges on the way to operation, since it was assembled on-site in 2011. The main problem is the age and origin of the turbine. As a nearly 30 year old design, documentation for the turbine itself and any third-party components can be difficult or impossible to locate. The third-party components



Figure 2.1: The Vestas V27 in Eveleth, MN

present an extra degree of difficulty as the unclear nature of their operation leads to the question of whether the component is damaged or simply misunderstood. Some of the signals seem to be encoded, with processing originally taken care of in the OEM Vestas controller. And there are potentially many components that are damaged in a turbine of this age, especially after shipping across the ocean, so a careful survey of all electrical signals and mechanical components was an essential part of bringing the turbine to operation. The students and instructors at Mesabi Range invested many hours repairing damaged components. These maintenance and repair tasks were essential for turbine operation.

The main control problem is the origin of the turbine. The turbine was shipped from Antwerp on September 28th, 2010. It was originally used at a wind facility in northern Europe, and designed to operate on the 50Hz electrical grid. Most of the turbine components are the same as the ones designed for the 60Hz grid, but the gearbox ratio for the rotor-to-generator connection is smaller, and the original control system was designed for this 50Hz operation. As it turns out, the original control system was deemed inoperable and removed from the turbine, so modification of the system was not an option. The turbine operation needs to be well understood as the

manual gives no operating values for a turbine running at this faster rotor speed. The turbine will, cautiously, operate at a higher RPM than its rated speed in order to make it produce power on the 60Hz grid. This can be done for the smaller generator in the initial design as the rotor speed will still be less than the maximum rated speed. The need for a higher operational speed is due to the way that an induction machine works, which is covered in section 2.2.

Once the turbine comes on-line, there are many possibilities for research. The current equipment allows for the testing of blade pitch control and yaw algorithms, which are heavily researched in the industry. This chapter covers a basic control algorithm for both the blade pitch and the yaw control in this thesis, although there is research being done for multi-input, multi-output control of turbines and wind farm optimization, both of which can be assisted by having this turbine available. MRCTC has a LIDAR which will allow for testing of wind and wake conditions of the turbine, which can be very useful for creating models of the turbine.

The use of this turbine is considered as a testing platform for the larger, more expensive, research wind turbine in Rosemount. The hope is that a testing procedure can be created for the Vestas V27 that will invoke confidence that researchers can safely and appropriately test control designs on the C96. This is a longer term goal, as the C96 is more in-line with modern wind turbine designs, and thus control efforts will be more true to industry needs on that turbine.

2.2 V27 Operation and Specifications

The Vestas V27 wind turbine is so named because of the 27 meter rotor diameter. The turbine is rated for 225kW at its maximum operational power, although it has a second generator for operation at 50kW in lower wind speed conditions. The turbine tower height is 30 meters with a rotor diameter of 27 meters, a maximum total height of around 45 meters. For a size reference, a single blade from the C96 turbine, coming in at 46.7 meters, would actually stand higher than the highest point on the Vestas V27 (Figure 2.2). More specifications for the turbine can be found in Table B.1 in Appendix B.

The V27 uses an induction generator, perhaps more properly referred to as an induction machine. This ‘machine’ terminology is used in order to emphasize the importance of this simple fact: the rotor-side, equivalent electrical frequency needs to be

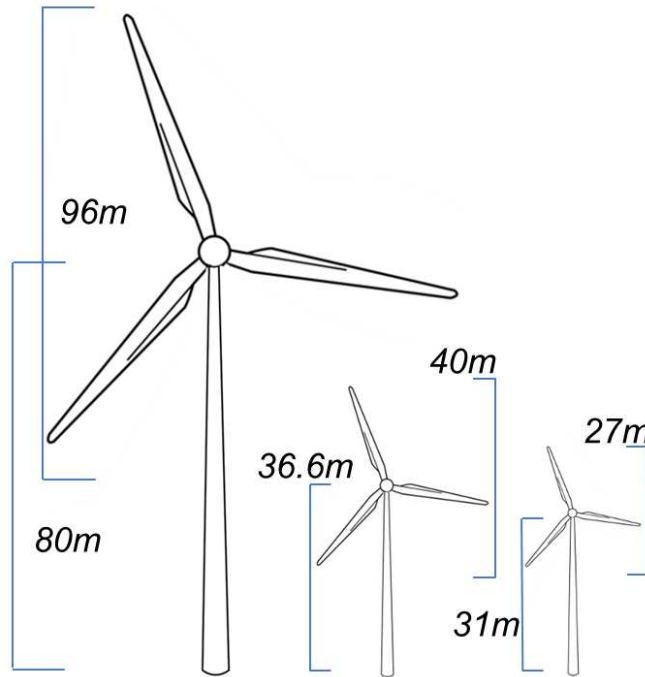


Figure 2.2: Left to right: EOLOS C96, NREL CART3, MRCTC V27

greater than the grid frequency in order for the turbine to produce electricity [13]. Below this nominal speed, the turbine would operate as a large fan, taking power from the grid. Induction machines usually specify their maximum operating rotational frequency within 1-2% of the nominal value, with the maximum difference corresponding to the rated power output. Outside of this range, the current is beyond the machine's rated value. For this reason, the controls of the turbine need to be very precise in the operating region.

It is also the reason why, at start-up, the turbine is not connected to the grid. The electrical grid cannot pull the turbine from a stalled state to the operating frequency. The wind is allowed to bring the turbine to the nominal speed without the loading electro-magnetic torque of the generator. This will motivate the design of the controller as presented in Chapter 3.

Generator specifications for the V27 as designed for the 50 Hz grid are included in Table 2.1. The rated generator rotational speeds presented in the table are for the maximum power operation point. The rated slip is 10 RPM for the 50 kW generator and 8 RPM for the 225 kW generator on the high-speed shaft for the 50 Hz grid. It

V27 Generator Specifications		
Type	Asynchronous Induction Type	
Number of Poles	8	6
Rated Power	50 kW	225 kW
Consumed Reactive Power	48 kVAR at 1/1 load	163 kVAR at 1/1 load
Voltage	400 VAC	400 VAC
Rated Current	101 A	396 A
Frequency	50 Hz	50 Hz
Nominal Generator Rotational Speed	750 RPM	1000 RPM
Rated Generator Rotational Speed	760 RPM	1008 RPM
Rotor Rotational Speed	33 RPM	43 RPM

Table 2.1: Generator specifications provided for V27 at 50 Hz [1].

should be noted that the rotor rotational speed, as given by the Vestas documentation, does not exactly agree with the generator rotational speed, and therefore it is likely an approximation. This rated slip is important as it determines the maximum power production of the induction generator. The requirement that this turbine operate at a the higher grid frequency means that everything is shifted to a different RPM. The nominal generator rotational speed for 60 Hz operation is 900 RPM for the 50 kW generator and 1200 RPM for the 225 kW generator.

It is difficult to say what this means for energy production on this turbine. For now, the goal will be to operate using the 50 kW generator only, as the nominal operational speed of 38.46 RPM on the low-speed shaft means that the rated speed will still be less than the maximum speed specified for 50 Hz operation. The turbine will be connected to the grid once it has reached the nominal frequency. Then the blade pitch controller will rely on current or power measurement in order to track the maximum power point. Perhaps after operational data is collected, the turbine control can be revised for frequency tracking.

One downside of this operation is that the turbine will operate with a higher tip speed ratio than it was originally designed for. This will likely mean a reduction in the efficiency of the turbine in much of Regions 2 and all of Region 3.

As mentioned in Sect. 1.3, a turbine with a power electronics interface to the electric grid can operate at variable speed, with the nominal operation speed chosen for

generator control. This is no less the case for this turbine, and should be considered as an option in order to expand the research capabilities. The generator control would have the added advantage of allowing the turbine to run at the optimal TSR despite the different grid frequency.

2.3 Subsystems

Several turbine subsystems are of great importance. An understanding of the various signals provided by the turbine and input to the turbine is required for designing any control system.

2.3.1 Blade Pitch System

The most critical control actuator for this turbine is the blade pitch system. This system consists of the blade actuator and the feedback signal for the blade pitch. The blade actuator is a linear amplifier connected to a hydraulic system. The controller specifies a voltage command for the amplifier, resulting in a commanded position for the hydraulic spool. This corresponds to a rate of flow in the hydraulic system, which moves a primary piston, resulting in the pitch of the blades. Therefore, the control system is really commanding a velocity for the change in blade pitch. In order for this system to operate, it is important that the blade pitch safety valve is closed and that the hydraulic motor is running. The pitch amplifier is shown in Figure 4.3 and the hydraulic motor is in Figure A.2.

The blade pitch sensor is a micropulse transducer. It operates in a manner that is analogous, yet opposite to the hydraulic spool command. An electrical pulse is sent down the line of this piston. The location of the blade pitch primary spool is marked by a magnet within the transducer. The magnet senses the electrical signal, and the propagation time of the pulse is computed. Within the transducer, this signal is then converted to an output voltage that the controller then measures. Besides the blade pitch sensor, the position of the hydraulic flow spool is measured by the amplifier system. This measurement may be useful for a MIMO control system.

2.3.2 Rotor Speed Measurement

The rotor speed measurement is a series of voltage pulses. There are 12 tabs around the rotor and as each passes a sensor, it produces a digital voltage pulse. A faster rate

of pulses corresponds to a higher rotor speed. The time between pulses is measured, then this value is inverted and converted from Hertz to degrees per second. The problem is that the pulses are quite noisy. There are two main issues with the signal noise: one is that a pulse will often turn off falsely and appear as two pulses, and the other is that there is sections of oscillating high-low signals that generally have only two barely distinguishable true pulses within.

The signal then required some processing in order to be useful. The first step was sensing the pulses. Data was collected and observed from the rotor speed measurement in order to determine what was expected for a pulse. A pulse seems to take about 1/6th of the length of a period, so any time a high signal appears of that length, it is likely a pulse. The result was filtered to drop the false negative within those pulses. It seemed like the signal only dropped for a single sample out of about 3 or more that corresponded to the true pulse. The piece of code used looked at the 3 consecutive samples and if the median sample was high, then the processed signal was true. This worked quite well in fixing the false negatives.

Then there was the issue of the scattered high-low noise. There wasn't really an easy way of truly distinguishing this noise from other pulses. The median filter used for the false negatives cleaned up a fair amount of the spurious high signals, but it was still clear from our view that it left some false positives in the processed signal. This was resolved by making the assumption that there wouldn't be a large change in the rotor speed in the range of only a couple samples. So if the time from the last pulse was less than half of what the distance between pulses was on the last sample, the new time was thrown out and the code continued counting until the next high signal. This seemed to do a fair job of finishing the pulse detection process.

The code was then converted into a Simulink real-time model, implemented in a Matlab function block. This initial design was done with a series of data that was all in the workspaces, so it was not yet causal. The processing was altered slightly to make the system causal. The final rotor speed was low pass filtered, balancing the need to reduce large variability with the need to stay true to the actual signal. The results, showing both the estimation of the actual pulses, as well as the filtered and unfiltered estimated rotor speeds are shown in Figure 2.3.

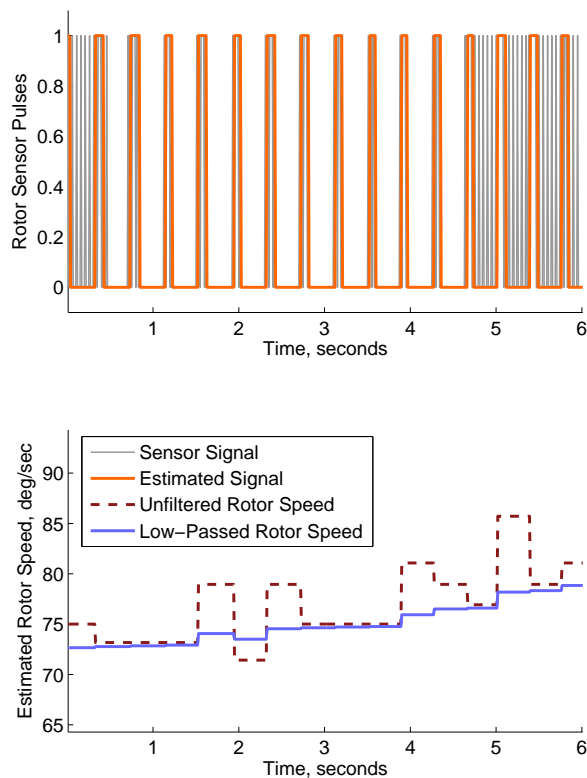


Figure 2.3: Estimating the rotor speed from the measurement signal.

2.3.3 Yaw System

The yaw system is tasked with rotating the nacelle and rotor system with respect to the prevailing wind direction. The turbine yaw motor is the actuator that controls the direction that the turbine is facing. The control for this actuator is two simple boolean commands to the yaw motor, one to yaw counter-clockwise and the other to yaw clockwise. The large mass of the hub and rotor means that the turbine yaws very slowly, approximately a half a degree per second. A full turn of the turbine would take 12 minutes at this rate. For the purpose of this control, this is fine, as the prevailing wind direction tends to be fairly static.

2.3.4 Anemometer and Wind Vane

The anemometer provides a measurement of the wind speed at the tower height. This can be put to use in some control situations, but due to the turbulence of this signal resulting from the rotor wake, this measurement is really only deemed accurate enough for use in the state machine operation. The anemometer is a wind capturing device with small cups that capture wind, causing the device to rotate around its vertical axis. It sends out a pulse as a magnet in the rotating part passes a stationary sensor, similar to rotor signal. A collection of pulses can be interpreted as a wind speed when the system is properly characterized. Getting a good estimate of the signal that corresponds to a specific wind speed is aided by the met tower data, logged directly beside the turbine. The data for the anemometer and for the met tower are not logged together at this time, but it will be useful when the anemometer wind speed estimate is tuned.



Figure 2.4: The anemometer and wind vane on the turbine nacelle.

The wind vane measurement is very important for system operation. The measurement provided seems to be the quadrant associated with the direction of the turbine rotor relative to the wind direction. The setting of these two bits corresponds to each of the four cardinal directions, relative to the turbine, or 90 degree increments for the error in the turbine's heading. It is troublesome to think that the only measurement available of the turbines heading is only accurate to 45 degrees of the desired heading. This will make the job of a yaw controller very difficult.

2.4 Hardware and Software

The design of the controls first required a look at the type of hardware and software that would be used to make the programming and application possible. The starting point was that it was desirable to use Matlab for the design of controllers, and then program onto a microprocessor-controlled FPGA called Compact Reconfigurable I/O (cRIO). The initial reasoning for use of the cRIO is that MRCTC had already purchased one for condition-based monitoring, pictured in Figure A.1. This controller required some interfacing software, and opens the possibility for more complicated programming processes.

2.4.1 Matlab for Control Design, Simulation and Development

Design in Matlab is common for controls applications, especially in academic circles. The Matlab/Simulink environment provides a relatively simple user interface and programming process familiar to most graduate and undergraduate students in engineering. Starting the design process in a familiar environment is a great advantage.

Within the program, there are several key processes that allow for clear programming, especially in this project. The first very attractive programming tool is the Simulink Stateflow toolbox. Stateflow allows for a user to see the process flow and the decision criteria for a control system. This is useful in a turbine because they function as state machines in their supervisory control systems. The designer can specify system states, define how the system transitions between the multiple states and set subsystem states that rely on the overall operating condition of the turbine. This is further assisted by the ability to call truth table functions and Matlab functions within the environment, allowing for a clean, uncomplicated look. Stateflow is used in the supervisory controller as well as in the yaw and blade pitch subsystems.

Simulink is well-designed for implementing control processes and studying the feedback systems. Users can specify state-space transfer characteristics, Laplace transfer functions, and develop subsystems that model linear and non-linear dynamics of any given system. In the case of this turbine, it is useful to feed collected turbine data into a linearized model of specific turbine dynamics, and tune the model in order to find the best possible match by comparing output graphs with real data. With the linearized model, the designer can then design and simulate control laws for stability and system performance, all within the same environment.

Design will be further assisted when the control designs begin to incorporate more complicated control designs. The Robust Systems Toolbox for Matlab is beneficial for the design and analysis of H_∞ and μ controllers for uncertain systems. This is useful due to the collective uncertainty of many of the system dynamics and noisy disturbances, such as the wind speed. Further analysis using these techniques will take place after the initial control design has verified confidence in the turbine structure.

2.4.2 Control Hardware

For the programming of this turbine, the decision was made to use the National Instruments Compact Reconfigurable Input/Output (cRIO) system. The system was found to be particularly useful for our needs due to the heavy duty build and reconfigurable nature of the device. The primary processor of the cRIO system is connected to a main chassis where different modular I/O devices can be installed for any number of desirable measurements and output signals. The cRIO systems are well understood by our partners at the St Anthony Falls Laboratory (SAFL), who have used the cRIO systems for multiple projects in conjunction with UMN researchers, including data collection from the Clipper C96. An engineer with SAFL helped MRCTC to set up a cRIO on the V27 for collecting data from strain gauges on the blades and tower. The system was familiar to all involved, and seemed to fit within the constraints of the project.

The current setup, pictured in Figure 4.3, includes modules for analog and digital input and output. The yaw motor, hydraulic motor and some other systems rely on the digital outputs, while blade pitch sensors and controls rely on analog input and output, respectively. These modules are all located on the same control chassis and connecting them to their corresponding turbine actuators and sensors requires only straightforward commands in the programming environment.

The cRIO system allows for operation in FPGA mode. This is a highly deterministic mode of operation, allowing for high speed and regular measurements. Currently all signals are directed through the microprocessor. This is fine for the operations that are required for this turbine controller. FPGA mode may be useful when data collection for feedback signals and other sensors is desired.

2.4.3 Control Software Implementation

The connection between the Matlab/Simulink design and the cRIO is greatly assisted by the use of National Instruments VeriStand. The primary use of VeriStand is incorporating real-time, deterministic software operations on the various National Instruments hardware. This program provides a conversion structure for Simulink to build a .out file which is then pulled into the VeriStand program. Within the VeriStand environment, the user specifies a programming target, and commands connections from inputs and outputs specified in the Simulink model to cRIO variables.

Once all the connections are made, the user selects a running frequency. Currently, the system is running the primary control loop at 100Hz, although this may need to be reduced if the control system requires a greater processing time. The actual running frequency can be monitored from the workspace. The cRIO is then programmed directly from the project window. The user can build a user interface in the workspace that includes boolean input and output, analog input and output, real-time plotting of desired signals and several other useful devices. The end product is a rather simply managed operating controller with the desired user capabilities easily accessible. The whole process is quickly implemented with practice, and basic but time consuming processes, like building a user interface, are usually carried over from previous designs, even when a controller is completely new.

This design process is further assisted by add-ons, such as the Scan Engine & Ethercat Engine which searches for connected hardware automatically. There is an add-on for data collection that makes the process for collecting data as simple as specifying the desired signals to be measured, then new files are created and data collection is controlled on the user interface, called the workspace. The functionality of the VeriStand and cRIO system can be expanded using custom tools developed in the LabVIEW programming environment. Sub-system operations that require a faster sampling rate or switching speed can be built and added in as asynchronous devices that run outside of the primary control loop (PCL). This kind of system can be useful for switching devices such as power electronics or pulse-width modulation systems that require higher frequency, variable speed operation that does not fit within the 100Hz bandwidth of the PCL.

2.5 Other Control Goals

Several control operations exist outside of this first primary design phase that will be studied further in future research. These include studies of blade and tower loading, frequency control and voluntary curtailment in Region 3 operation. Studies of loading and the control laws that attempt to mitigate this loading are assisted by existing strain gauges, as well as the LIDAR and MET tower data available at the Mesabi location.

Further research is being done on turbine interactions in a wind farm. The current goal for wind farms is to make them much more like conventional power plants. This requires that the system operate in such a way that it can capture the maximum amount of power available in the wind, and to reduce the power output as commanded by the independent system operator. Current studies are looking at blade pitch and generator torque control for system and individual turbine curtailment, and yaw control for directing turbine wakes in order to reduce wake interactions with the next turbine downwind [4].

Chapter 3

Control Design

This chapter will describe the design process taken for the different elements of the turbine control system. The design was guided by original Vestas documentation for the turbine, knowledge of desired traits of turbine operation, and desired characteristics for controls research. Basic system requirements were derived from Vestas V27 documentation [1], [11]. as well as the existing literature on the more modern C96 turbine design. Designs were formulated, tested in simulation, and finally implemented and experimentally tested on the Mesabi Range V27 turbine.

3.1 Programming and Testing Interface

The basic user interface for the turbine controller is created in the VeriStand workspace. The workspace allows the selection and monitoring of Boolean and double signals, as well as active operations such as graphing of selected turbine signals.

Design and testing of controllers for the turbine took place remotely. The interaction with the Compact RIO took place through a Remote Desktop connection to a server located at the MRCTC campus. The view of the programming interface is shown in Figure 3.2. The turbine was monitored via web cam and the image was displayed, along with the VeriStand workspace, on the desktop of the Pi server.

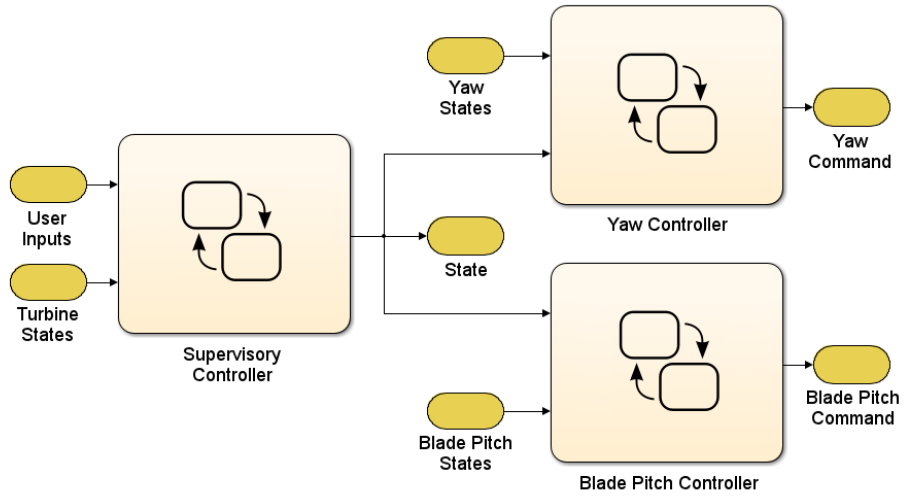


Figure 3.1: A simplification of the control architecture implemented in Simulink.

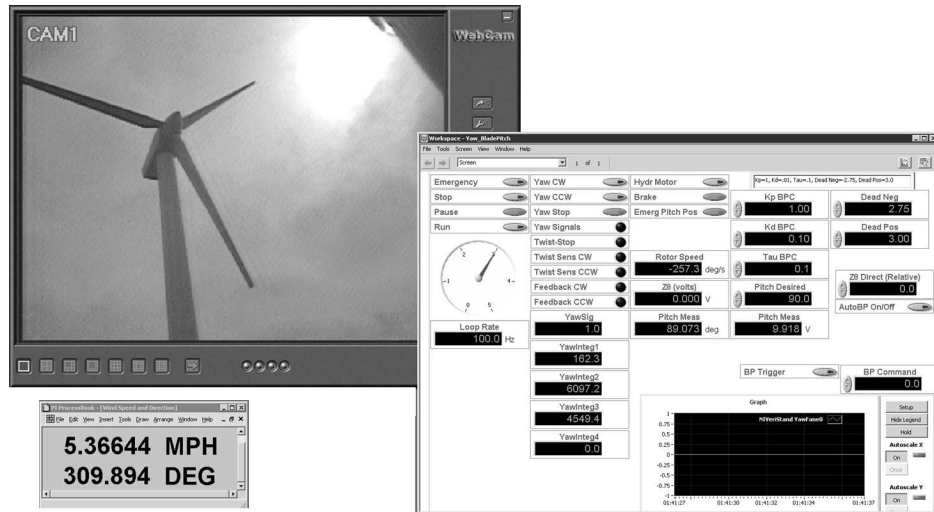


Figure 3.2: The testing interface, showing VeriStand and the V27.

3.2 Supervisory Control

The supervisory control tracks the status of the system, provides an interface with the operator, and sends commands to lower level subsystems, e.g. the blade pitch and yaw control subsystems. The interaction of the supervisory control with the user and lower level subsystems is shown in Figure 3.1.

The turbine has four clearly discernible operational states. The four states are Emergency, Stop, Pause and Run, in that order. The desired state is selected by the user, but transitions into those states are dependent on the operating conditions. The turbine may only increase one state at a time to reach the final run state. However, it is possible for the turbine to immediately step downward through multiple states depending on the situation. Each of these states has its own desired conditions and functional capabilities. A Simulink implementation of the designed supervisory control is shown in Figure 3.3. Details on each state as well as the transition logic are provided in the following sections.

3.2.1 State: Emergency

The first state of concern is the Emergency state. Emergency is the default state of the system. The basic requirement of Emergency, as described in the Vestas manual [11], is that every operation of the turbine come to a standstill. The desired state for the turbine subsystems is parked, meaning that it is yawed with the rotor parallel to the wind flow and the blades are pitched to the feathered position, 90 degrees. The parking brake is applied to complete the operation. The user is not allowed to manually yaw or pitch the blades. No power is produced in the Emergency state, and the generator is completely disconnected from the electric grid.

Transitions to and from Emergency are determined by multiple factors. Transitions to Emergency can take place because of a user command from inside the turbine or from the user interface. Unsafe conditions, e.g. turbine overspeed, will also cause a transition into Emergency. Following a transition into the the state, the turbine is held for 1 minute before a transition up can occur, a condition added for safety purposes. Transitions out of the state require a command for a higher state from the user interface.

The Emergency state is designed to handle cases of operational failure and for keeping

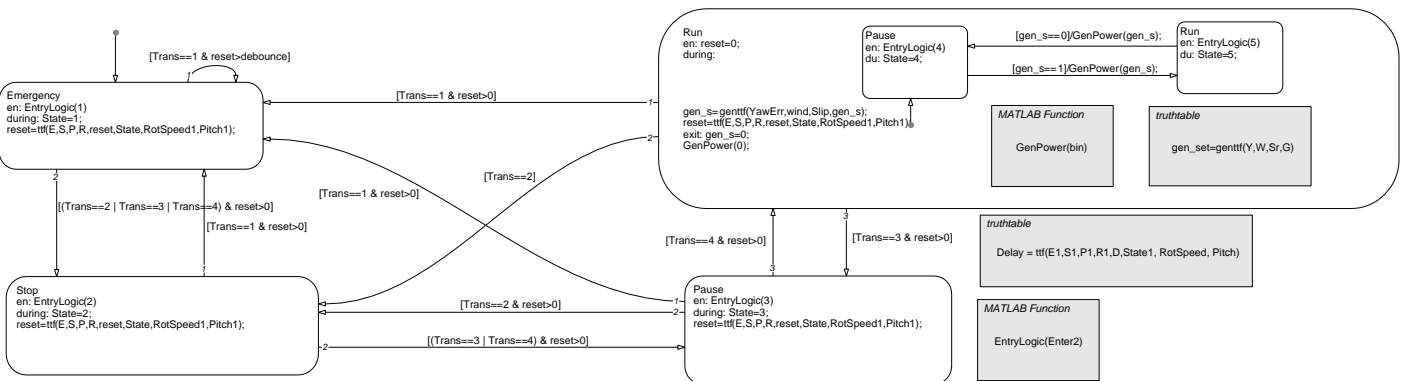


Figure 3.3: Supervisory controller structure as implemented in Stateflow.

the turbine static should a technician need to access moving turbine components. One of the manual suggestions is that the blade pitch hydraulic valves be opened, which would immediately feather the blades. Careful consideration needs to be given for what is expected of transitions into the Emergency state. The desired condition is parked, but transition to a parked state requires motion of both the blade pitch system and the yaw system, both of which are implicitly forbidden in the documentation. If the need to transition to Emergency allows for it, the turbine should step down to the Emergency state via the intermediary states, Pause and Stop.

3.2.2 State: Stop

The next state following Emergency is Stop. This state differs from its predecessor in that it is not required that the turbine remain motionless. The desired subsystem states are still that the turbine be yawed 90 degrees out of the prevailing wind direction with the blades fully feathered. However, the brake is off in this state which allows the rotor to turn freely. No automatic yaw control or blade pitch control occurs in this state. The state allows for manual yaw but not for blade pitching, as the full-feather valves on the hydraulic system are still open.

Transitions to Stop from Emergency require that the user command a state greater than or equal to Stop, that the turbine has cleared all faults that would cause a transition to Emergency, and that the emergency delay period has passed. Transitions from higher level states could occur for many reasons, most commonly a command from the user. Entry in to Pause would require no extra clearance other than a user command. It is only within Pause that transitions into those desired states would occur.

The Stop state is mostly an intermediary between the more distinguishable states of Emergency and Pause. Again, transitions down into this state should be carefully considered. No automatic yaw will occur, but the full-feather valves will bring the blades back to the parked position. The turbine should step down through the Pause state if possible.

3.2.3 State: Pause

Pause is a more active state. The turbine still operates with the goal of minimal capture, meaning that the desired state for the subsystems is the parked position.

However, the turbine is now active in maintaining this desired state. Automatic yaw and blade pitch both occur in this state to maintain the heading out of the primary wind direction and to keep the blades feathered. This requires that the hydraulic motor maintain active pressure with the full-feathering valves closed. The brake is off. Manual yaw and blade pitch are both allowed in this sub-state.

Transitions to Pause from Stop only require a user command and that no errors are present that would require a transition down to either Stop or Emergency. The transition from Run will take place with a user command. This may be a good state to transition to in case of turbine over-speed, as a transition to Pause would pitch blades to the parked position and yaw out of the wind without the more serious results of a transition to Stop or Emergency.

This state is useful for actuator testing. The user can command a blade pitch or a desired rotor speed within this state, as well as a yaw direction. The state has been used when characterizing the blade pitch actuators and in testing of the various sub-system controllers that have been implemented on the Mesabi V27. Pause is much like the staging area for the Run state. The turbine is yawed out of the wind and blades are feathered, but all of the turbine subsystems are functioning, leaving it very close to the active state.

3.2.4 State: Run

The functional state of the turbine is the Run state. The desired condition in this state is one that enables maximum power production. The turbine yaw controller keeps the rotor facing directly into the wind. The blade pitch controller is tracking to rotor speeds that will allow for production of power.

A transition to the Run state only requires a user decision to enter into the Run state. It may be useful to include a minimum wind speed threshold for entry into the state in order to avoid unnecessary actuation of the blade pitch system. Transitions away from the Run state are all transitions downward, and therefore all take priority to the Run state. Any user command of another state or a system error will result in a transition away from Run.

The Run state is implemented as two different sub-states, one that is producing power and one that is not. The goal of Run is always to produce power, but there are quite

a few requirements in order to get the turbine to that point. The most optimal way to do this seemed to be with the sub-state structure as it simplifies the way a transition to a lower state would be handled should the turbine be in the non-power producing sub-state. The non-power producing sub-state, which I will refer to as Run.1, is the entry state of the Run block. In this sub-state, the blade pitch controller attempts to get the generator electrical frequency to match the grid frequency.

In order to produce power, some requirements need to be fulfilled: the wind speed needs to be above the cut-in wind speed, the blade pitch controller must be tracking the rotor speed corresponding to the grid frequency, and the system ought to be error free. The system will then be allowed to transition into Run.2. This is the power producing sub-state of Run. Upon entry, the thyristors are closed, allowing the stator windings to connect with the grid. The rotor tracking controller then changes in order to attempt to track the rated rotor speed. It would be within this Run.2 state where considerations of Region 2 and Region 3 control objectives would take place.

3.3 Blade Pitch Control

Blade pitch control is an extremely important facet of the turbine operation. It is the most complicated of the control systems, as well. Blade pitch control is necessary for tracking rotor speed which is the power control for the turbine. This control subsystem is only active in the Pause and Run states.

3.3.1 Blade Pitch Subsystem

Achieving the desired rotor speed will be a difficult task for the turbine that will require a sub-state structure. The rotor speed responds to the blade pitch in a manner that is highly dependent on the wind condition and the current rotor speed. Only at rotor speeds that are above half of the rated speed will the turbine seem to speed up, assuming favorable wind conditions, if the pitch is close to the trim condition. The turbine actually responds more to torque at the lower rotor speeds, which allows the rotor to gain momentum more efficiently. In fact, leaving the turbine at the trim condition at low rotor speeds usually results in a stall. Therefore, it makes sense to include a sub-state structure that will guide the turbine through this turn-on process.

This state machine, shown in Figure 3.4, is tasked with commanding a desired blade pitch. Other inputs include the state from the supervisory controller, the control

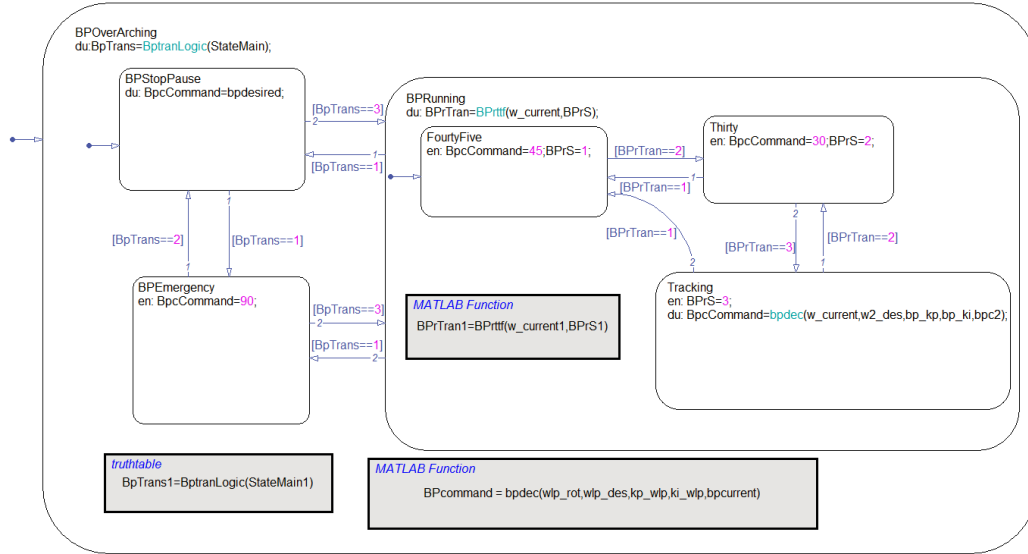


Figure 3.4: The blade pitch command state subsystem.

weights and a desired blade pitch for manual control. The blade pitch command is then sent to an inside control loop that pitches the blades to the desired position.

This turn-on sub-state would be active immediately upon entering the Run state. Run.1 operational states are dependent on the rotor speed, but the attempt is to follow the blade pitch for a portion of it. The initial state commands a blade pitch of 45 degrees, allowing the turbine to gain momentum. This state is constructive as the rotor speed measurements tend to be blatantly inaccurate at low rotor speed. The next state would pitch the blades to about 30 degrees, allowing the turbine to speed up further. Each of these would have a threshold for the rotor speed that would allow a transition to the next sub-state: 80 degrees per second for 45 degrees pitch, 140 degrees per second for 30 degrees pitch, and 200 degrees per second for 15 degrees pitch. These may need to be adjusted based on prevailing wind. The final sub-state would be the running state where the blades are controlled to track rotor speed.

3.3.2 Pitch Controller Inputs and Outputs

Referring to Figure 3.5, the two primary input signals to the control system are the blade pitch measurement, β_{meas} , and the rotor speed measurement, ω_{meas} . The rate of pitch is available as a voltage measurement indicating the hydraulic actuator valve position, however that may only be used in more advanced control systems.

The blade pitch measurement signal is an analog voltage between zero and ten volts that corresponds linearly to a blade pitch. The signal is only slightly noisy, and thus little processing is required to estimate the pitch, β_{est} degrees. The rotor speed measurement required more thorough processing, detailed in Section 2.3.1, and the resulting estimate is given as ω_{est} . S1 and S2 are sensors and P1 and P2 represent processing in the controller.

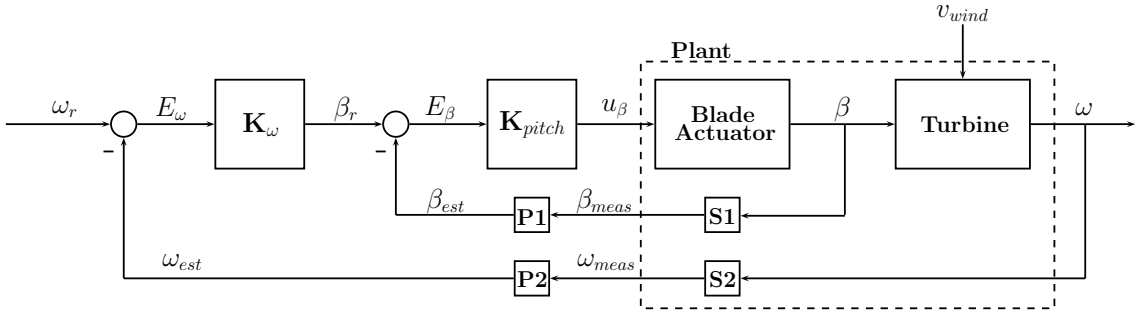


Figure 3.5: Closed-loop blade pitch system.

The control signal, u_β , is a voltage corresponding to the rate of change of the blade pitch. This is an important distinction from commanding a blade pitch. The voltage sets a position for a hydraulic valve, which corresponds to a rate of flow in the hydraulic circuit, which is a velocity of the arm that rotates the blades. It is for this reason that the system between the actuator signal and the output blade pitch, β , is modeled as an integrator cascaded with a low-pass filter for the purpose of initial control design. The transfer function for the model actuator is given in Equation 3.1.

$$\beta = \frac{C1}{s(\tau s + 1)} \times u_\beta \quad (3.1)$$

3.3.3 Blade Pitch and Rotor Speed Tracking

Until recently, the blade pitch sensor was thought to be faulty. The signal that was returned from the device was incomprehensible. Due to the fact that a rotor speed measurement was available, a proportional controller of the blade pitch was still implemented with the desire of tracking a specific rotor speed. The design was done with the fairly simplistic estimate of the actuator transfer function in Equation 3.1, and a similar estimate for the transfer function to rotor speed. The resulting control loop was very lightly damped. Results for this test are shown in Figure 4.2.

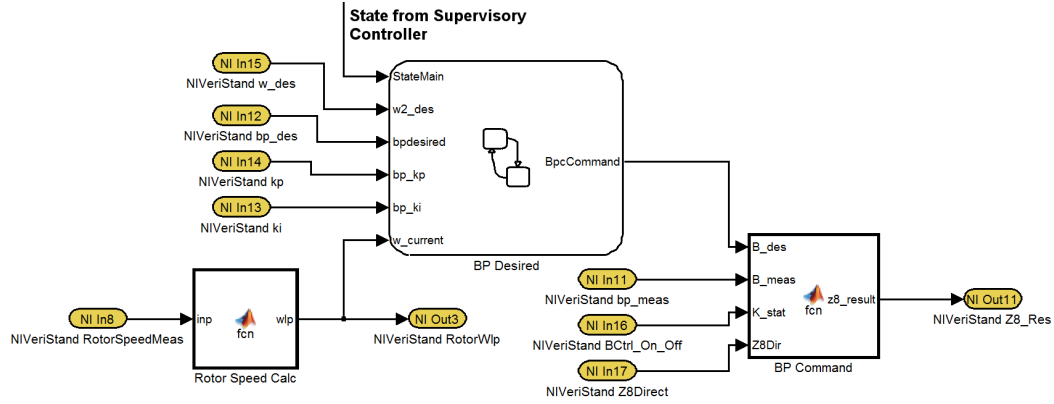


Figure 3.6: The full blade pitch subsystem.

This was a complicated task for several reasons. Without the blade pitch sensor, it is very possible to saturate the blade pitch position. The blades pitch much faster than the rotor speed can respond in most wind conditions. This will cause problems if one tries to implement an integrator term in the control law, and integrator anti-windup is not possible without knowing that the pitch has been saturated. The need for a start-up blade pitch as described in Section 3.3.1 further complicates the issue.

The problem above could be an interesting motivation for future research. A common goal of researchers in controls is operating systems in the case of an actuator or sensor failure. In the case of wind turbines, allowing the turbine to operate despite the loss of the blade pitch sensor would result in more earnings from the turbine because of reduced operational down time.

With the blade pitch sensor operating, the design is more clear. The rotor speed tracking system sends a blade pitch command to the blade pitch inner-loop. The turbine responds to the blade pitch, β , and the wind disturbance, v_{wind} , and the estimate of the rotor speed is fed back in to the rotor speed controller. The system as implemented in Simulink is shown in Figure 3.6.

This first required implementation of the blade pitch inner-loop. Using loop-shaping techniques for SISO systems, a controller was designed in Simulink and tested on a model using the assumption in Equation 3.1. The gain and deadband of the actuator are accounted for when commanding the actuator voltage, u_β .

The blade pitch tracking is implemented with a PD controller, and tuning of the

controller took place from within the VeriStand workspace. The gains and roll-off time, K_p , K_d and τ , were available as user inputs during the testing period of the controller. Adjustments to the controller gains were made in order to stabilize the resulting actuator command.

Due to errors in the assumptions about the actuator transfer function, tests were run to better characterize the blade pitch actuator, as detailed in Section 4.3. This allowed construction of a better model of the blade pitch controller for the purpose of control design.

3.4 Yaw Controller

The yaw system of the turbine consists of a single motor that turns the turbine rotor relative to the prevailing wind direction. The system is the largest of the actuators. After a fair amount of inspection, the turbine seems to be capable of yawing at rate of only about .5 degrees per second in either direction.

The yaw system has a few requirements that should be understood. The automatic yaw controller should be able to follow the desired yaw direction with some minimal amount of fidelity, perhaps erring no more than 15 degrees for more than 20% of any 10 minute period. Because of the slow actuation, the yaw controller will not be able to respond to fast changes in the wind direction, and instead is set to respond to an average wind direction. The user should be able to command a yaw in either the clockwise or counter-clockwise direction, or halt the yaw if desired. This is beneficial for general controls testing, maintenance, and requirements for the schools technician program.

Finally, the system requires a sensor that will force the turbine to unwind after a set number of rotations. The cables in the turbine tower are only designed to twist a finite number of times before incurring damage. This corresponds to about 2.5 turns in either direction, and the turbine should then override any automatic or user yaw command and start the process of yawing towards the zero condition. These requirements fit well with the use of another sub-supervisory state machine that deals with the hierarchy of these needs.

Chapter 4

Testing and Results

Implementation of the control system on the Mesabi V27 required the testing of each component. Testing occurred with user commands in the VeriStand Workspace. Results were collected using the VeriStand data-logging add-on, Embedded Data Logger. Signals are specified in the System Definition File, to be logged at 100 Hz, and logging is controlled from the Workspace. The results were downloaded from the cRIO and processed using Matlab.

4.1 Rotor Speed Tracking

As was detailed in Section 3.3.3, the first controller designed for tracking rotor speed lacked a blade pitch measurement, which puts the turbine at risk of actuator saturation among other issues. Although no inner-loop controller for the blade pitch was available, it still seemed appropriate to try to track rotor speed, at least when the turbine had already been brought up to a reasonable speed. A simple proportional controller with adjustable gain was installed on the Mesabi V27, modeled in Figure 4.1.

Shown in Figure 4.2 are the results for attempting to maintain the operating speed. As can be seen, the loop is clearly very lightly damped and the response is more oscillatory than desired. Although not necessarily dangerous, the oscillations were large enough that the system was disconnected immediately from the rotor tracking controller, and the turbine was returned to a parked position using a user command of the pitch actuator voltage.

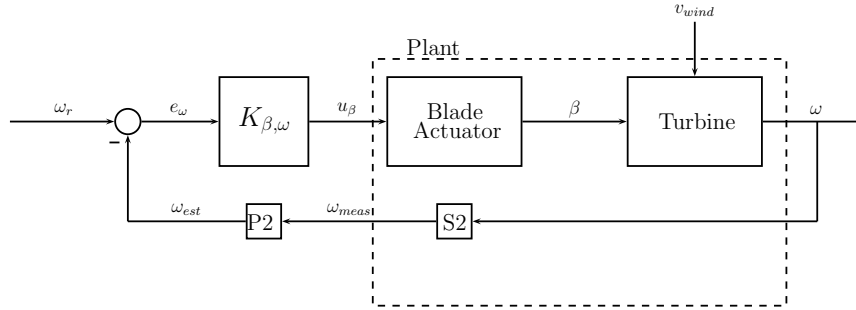


Figure 4.1: Closed-loop rotor speed controller without blade pitch sensor.

The test was based on some assumptions regarding the system, some of which have been proven incorrect. The first transfer function from actuator voltage to blade pitch was modeled as an integrator with a roll-off, and the second from blade pitch to rotor speed as a low-pass filter. Gains and poles were chosen based on observations. The pole for the second transfer function was thought to be at low frequency due to the large inertia of the rotor. These assumptions seem to be correctly based, but the gains and time constants chosen did not prove effective. However, the actuator deadband was set to -4 volts and 4 volts, which likely caused some of the oscillatory behavior.

The experiment proved the need for a better characterization of the transfer functions in the blade pitch system and to the rotor speed. Shortly following this test, the blade pitch measurement became available and focus immediately turned to creating the inner-loop controller for the pitch angle. It would be of interest to continue experimenting with a rotor speed controller that lacked a blade pitch controller following a better analysis of the system dynamics.

4.2 Modeling the Blade Pitch Actuator

The input to the blade pitch actuator is a voltage, which is then processed by the Vickers amplifier shown in Figure 4.3. This results in a command for a position of the hydraulic valve spool. Motion of the valve spool controls the flow of the hydraulic fluid which corresponds to the rate of blade pitch. A convenient model based on this information is given in Equation 4.1, where u is the voltage signal to the actuator and β is the blade pitch.

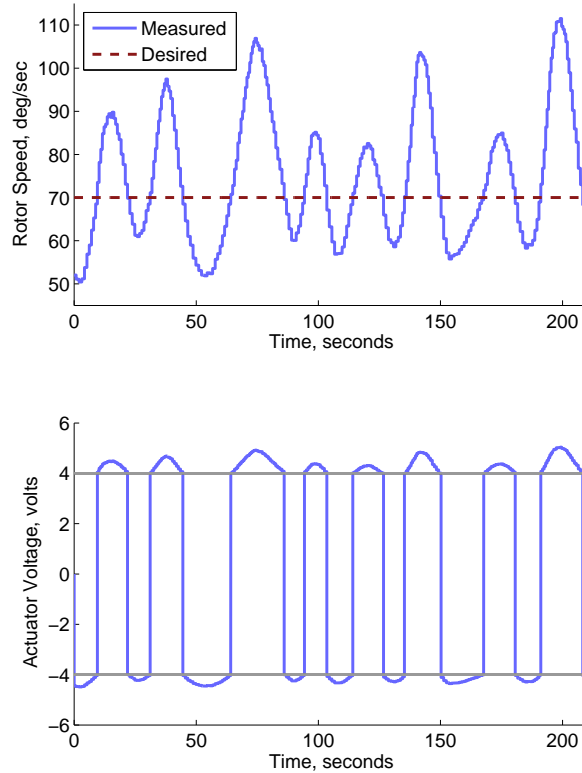


Figure 4.2: Step command of desired rotor speed, no blade pitch inner-loop.

$$\frac{d\beta}{dt} = f(u) \quad (4.1)$$

It was understood that the pitch system had a deadband where a commanded voltage, u , would not result in any movement of the blades. It was difficult to determine if the blades were pitching based on sight, but an initial estimate for the deadband and the rate of pitch was made. A model of the actuator was created assuming that the deadband was between -3 and 3 volts and the gain was estimated to be 3 degrees per second per volt beyond the deadband. Based on this model, a proportional-derivative controller for tracking a reference blade pitch was developed and tested as described in Sections 3.3.3 and 4.3.

Although the blades tracked the reference pitch with low steady-state error, the result was troublesome. The actuator voltage input, u , oscillated between the rails of 8 and

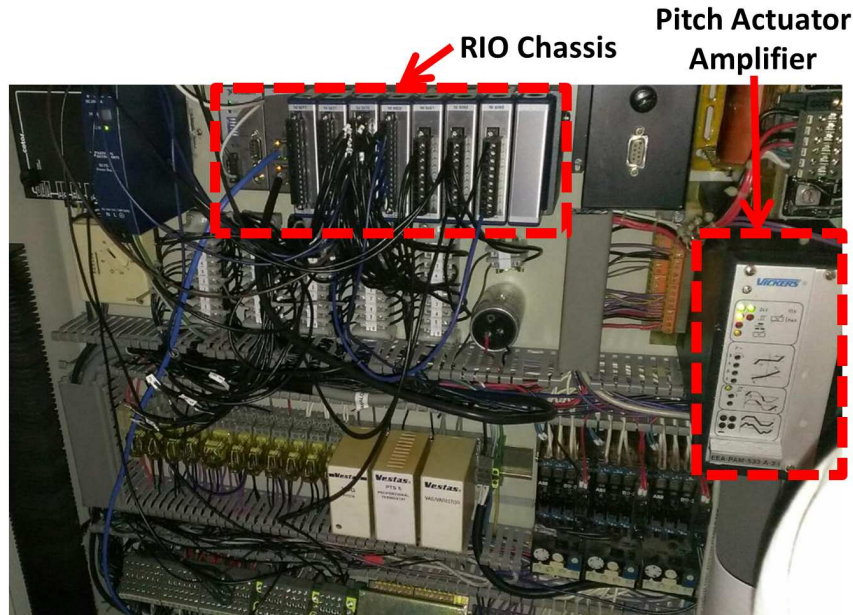


Figure 4.3: The cRIO in the nacelle, and pitch actuator amplifier.

-8 volts. The problem was solved by reducing the derivative gain, K_d , however it motivated testing to better characterize the pitch actuator.

An experiment was performed to further understand the blade pitch actuator. The results showed that the deadband goes between -2.75 volts and 3 volts. The slope is approximately the 3 degrees per second per volt that was assumed before.

The experiment was run as two separate tests. The first characterized the pitch from the parked position, 90 degrees, to the trim position, 0 degrees. A negative pitch velocity requires a negative command voltage. The second went the opposite direction and required a positive command voltage. The voltage was incremented by hand in steps of .05 volts about as fast as it could be done until the actuator saturated at the trim or parked position, respectively. This only covered the range between -7.5 volts and 7.5 volts, but this seemed to be a good indicator of the actuator functionality. It appeared that the velocity was not dependent on the pitch angle.

In Matlab, the *diff* function was used to find the average rate of change of blade pitch, which was compared to the change in voltage. There were many samples available at each voltage as the logging frequency is faster than human response. The plot showing the transfer from actuator voltage to the average pitch rate is shown in Figure 4.4.

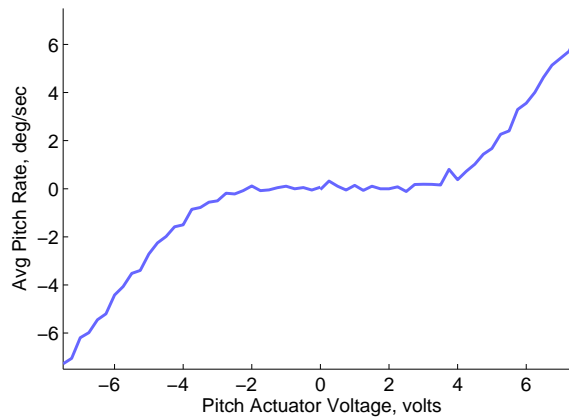


Figure 4.4: Characterizing the blade pitch actuator.

4.3 Blade Pitch Tracking

As detailed in Section 3.3.3, the first test of blade pitch tracking was done with a PD controller using assumptions made from observation. The designed plant was based on the assumption that the pitch rate gain is 3 and the dead-band is from -3 volts to +3 volts. The proportional gain, K_p , and derivative gain, K_d , were set to 1 volt per degree and 1 volt per degree per second, respectively, and the roll-off for the derivative gain was 10 Hz, $\tau = .1$ seconds. The results for a step change in the reference blade pitch are shown in Figure 4.5.

The system tracks to the desired blade pitch well. The steady state error is minimal, and the overshoot is minimal as well. However, the control signal oscillates between the positive and negative rails. It seems to be suffering from sensor noise amplification due to the relatively large value of K_d . Although not an unstable controller, this kind of actuator saturation is undesirable.

The original controller allowed the user to select the controller gains from the VeriStand Workspace. This allowed more tests to be run after altering the various gains, without the need to re-program the cRIO. The controller was adjusted such that $K_p = 1$, $K_d = .01$ and $\tau = .1$, while the rails were adjusted to -2.75 volts and 3 volts. Results for a test performed are shown in Figure 4.6. The response is very similar to the last test. The blade pitch tracks to the desired pitch angle at a rate of about 6 degrees per second. There is a very small overshoot, approximately 1%, and then the angle settles with a negligible steady state error. The response of the pitch actuator

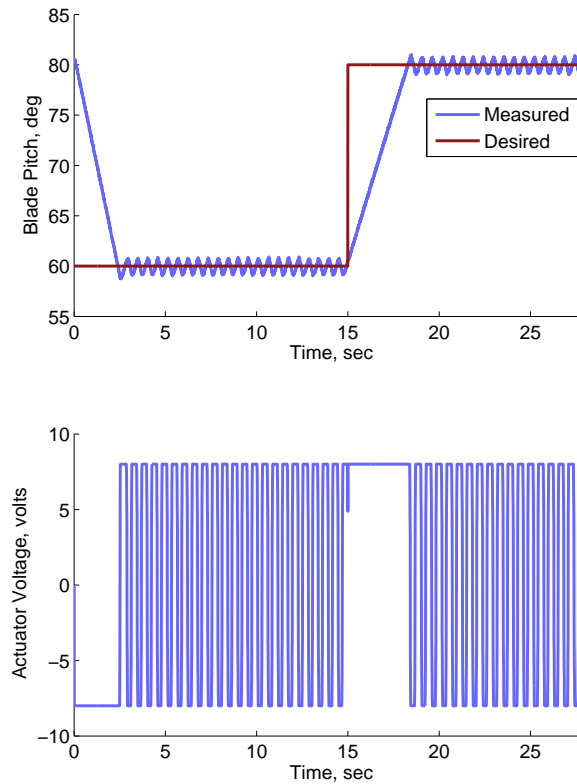


Figure 4.5: First step for blade pitch reference tracking.

voltage is much better. The voltage signal saturates as it climbs immediately following the step. But in steady state operation, the signal merely oscillates a half volt to either side of the rails. This is presumably just a response to noise in the blade pitch sensor. The result indicates that the blade pitch controller can operate reliably with a simple PD controller.

4.4 Modeling the Turbine Rotor

The attempt was made to run experiments that would allow for better modeling of the transfer function from blade pitch and wind speed to the rotor speed. Although not encompassing the needs of system modeling, the results are a good starting point for this goal. A better model of this system will allow for the development of better rotor speed controllers.

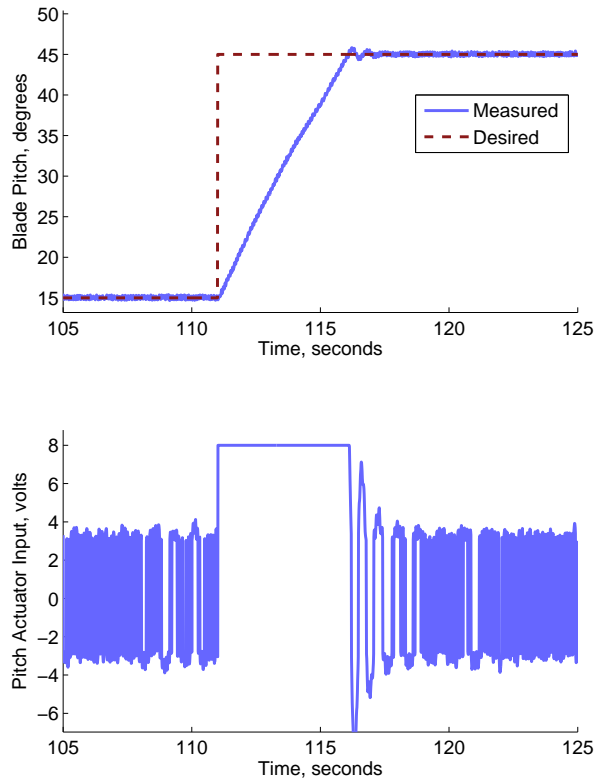


Figure 4.6: Second step for blade pitch reference tracking.

The assumption was that the transfer function between the wind speed and rotor speed and between blade pitch and rotor speed are both low pass filters, with poles probably around 1 Hz. Results showing the response of the rotor speed for step changes in blade pitch are shown in Figures 4.7 through 4.9. The wind speed was noted based on the measurement from the meteorological tower beside the turbine.

The test results in Figure 4.7 show a step change in blade pitch from 30 degrees to 20 degrees. The wind speed was between 2 and 3 meters per second. An attempt was made to allow the rotor speed to settle before commanding the blade pitch, however the speed was decreasing when the step came.

The rotor speed increases with the appearance of a first-order transfer function as expected, however the wind speed appeared to be playing a role in the response and the rotor speed did not settle as expected. Approximating the actual measurement

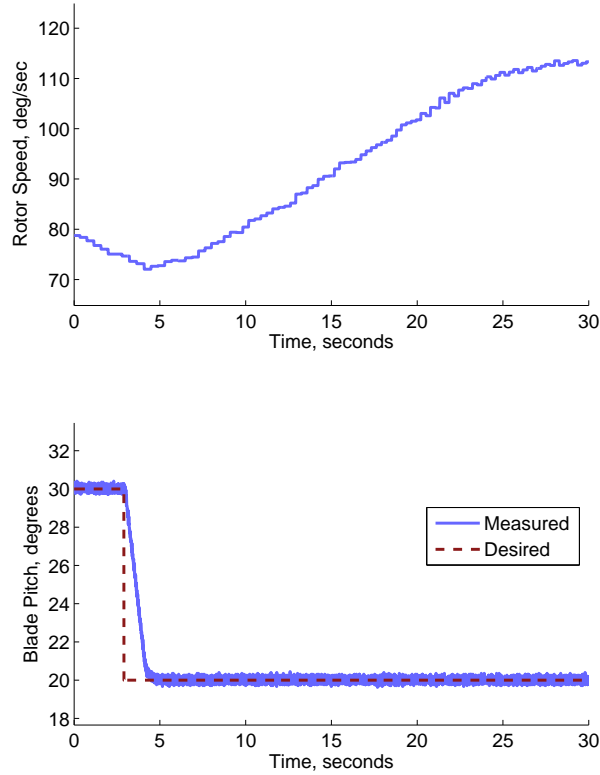


Figure 4.7: Rotor speed response for a step change in blade pitch. Test 1.

as an ideal step at $t \approx 5$ seconds, it would appear that the rotor speed goes from 75 to 110 degrees per second, with a settling time of 20 seconds. This implies that the turbine dynamics at the given wind conditions have a time constant of ≈ 6.6 seconds, which corresponds to a pole at $1/6.6$ radians per second. This is quite far from the initial approximation of a 1 Hz pole. The transfer function can be approximated as in Equation 4.2. Together with the results of the other two tests, this may be useful in determining a system model.

$$\frac{\delta\omega}{\delta\beta} = \frac{3.5}{6.6s + 1} \quad (4.2)$$

The test results in Figure 4.8 show a step change in blade pitch from 15 degrees to 45 degrees. The wind speed was between 3.2 and 5 meters per second. As can be seen in the top of the figure, this change in rotor speed resulted in a massive deceleration

of the turbine. The rotor speed went from 118 degrees per second to less than 30 degrees per second in about 15 seconds. Again, due to an observed decrease in the wind speed, the rotor speed for the final settling will be approximated as 30 degrees per second. The transfer function can be approximated as in Equation 4.3.

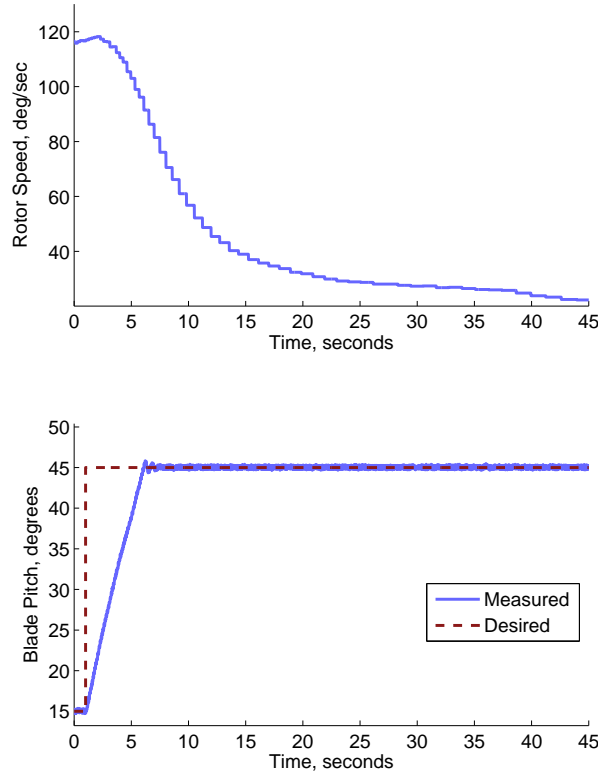


Figure 4.8: Rotor speed response for a step change in blade pitch. Test 2.

$$\frac{\delta\omega}{\delta\beta} = \frac{3.0}{5s + 1} \quad (4.3)$$

The response here was faster than in the first test. This is possibly due to the large amount of extra drag created by the blades at 45 degrees pitch. This may have contributed to the continuing decrease in the rotor speed following the estimated steady state.

The test results in Figure 4.8 show a step change in blade pitch from 15 degrees to 45 degrees. The wind speed was between 3.2 and 5 meters per second. The wind

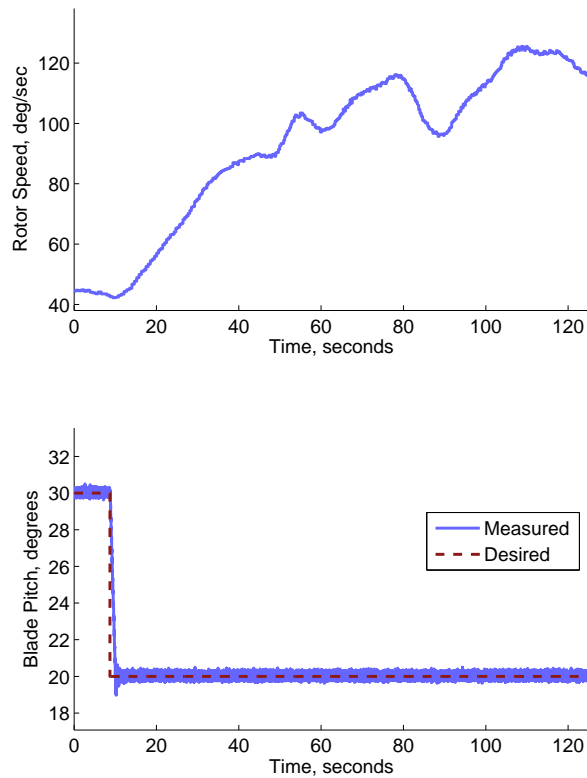


Figure 4.9: Rotor speed response for a step change in blade pitch. Test 3.

was quite turbulent over the period of the test. It shows that the tests here are quite susceptible to changes in the wind speed. No attempt will be made to derive a transfer characteristic from this result.

The first two results seemed to indicate that the gain between blade pitch and rotor speed is about 3 degrees per second per degree of blade pitch. However, this result is only valid at a wind speed of 3 meters per second. More testing will need to take place before an accurate model can be obtained for various wind speeds.

Chapter 5

Conclusions and Future Work

A control structure for a Vestas V27 was presented. The design process included within was motivated by requirements for turbine operation, as well as for future research. The system was designed and tested using the StateFlow toolbox in Simulink, then programmed on to the Mesabi V27 using VeriStand. The programming process was simplified, allowing for incredibly quick re-working of the system. The design was verified through initial data collection and sub-system control implementation.

Wind turbine control systems are being considered using more advanced control algorithms and prediction systems. Active and reactive power control and blade load mitigation makes research in the turbine controls academic communities of increasing importance. Development of the controller for this Vestas V27 opens many possibilities for researchers for testing blade pitch systems and verifying turbine modeling techniques. There exists a market for used turbines could benefit from a simple control design such as the one provided here-in.

There are a few more tests that should take priority in the continued design of this turbine controller. These cover all of the control subsystems. A controller for the blade pitch should be developed that uses more of the capability of the actuator. Currently, the control signal is set to saturate at -7.75 volts and 8 volts. The input to the actuator can accept up to 10 volts on either rail. This test has not been run yet due to concerns regarding the speed at which the blade pitch might saturate. However, with a proper controller, this concern could be mitigated. The new controller should be designed carefully so that it either uses the derivative control, or it is not a part

of the system. With the derivative gain set so low, it is possibly of very small use in the current control design. Additional model verification can occur in Matlab that will lead design of the controller.

Finally, a better model of the turbine plant needs to be developed. The best way to do this might be to investigate the $C_p(\lambda, \beta)$ curve, resulting in a non-linear model of the system. This would allow the linearization of system dynamics at many different operating points. The result would be a better characterization of the system response to changes in both the blade pitch and in the wind speed. This modeling will be greatly assisted by collection of data for the wind measurements. The process of importing data from the MET tower to the cRIO for logging beside the rotor speed data is still in development. The inclusion of this data, however, should be a high priority as testing continues.

Bibliography

- [1] Vestas, *General Specification: Vestas V27-225 kW, 50 Hz Windturbine with Tubular/Lattice Tower*, VESTAS, Aarhus, Denmark, 1st ed., 1994.
- [2] “EOLOS Wind Energy Research Consortium,” <http://www.eolos.umn.edu/>, May 2013.
- [3] Johnson, K., Pao, L. Y., Balas, M., and Fingersh, L., “Control of variable-speed wind turbines: standard and adaptive techniques for maximizing energy capture,” *Control Systems, IEEE*, Vol. 26, No. 3, 2006, pp. 70–81.
- [4] Johnson, K. E. and Thomas, N., “Wind farm control: Addressing the aerodynamic interaction among wind turbines,” *2009 American Control Conference*, 2009, pp. 2104–2109.
- [5] Pao, L. Y. and Johnson, K. E., “Control of Wind Turbines,” *IEEE Control Systems*, Vol. 31, No. 2, April 2011, pp. 44–62.
- [6] Wiser, R. and Bolinger, M., “2011 wind technologies market report,” Tech. Rep. August, U.S. Department of Energy, 2012.
- [7] Aho, J., Buckspan, A., Laks, J., Fleming, P., Jeong, Y., Dunne, F., Churchfield, M., Pao, L., and Johnson, K., “A Tutorial of Wind Turbine Control for Supporting Grid Frequency through Active Power Control,” *Proceedings of the American Control Conference*, 2012, pp. 3120–3131.
- [8] Manwell, J., McGowan, J., and Rogers, A., *Wind Energy Explained: Theory, Design, and Application*, Wiley, 2010.
- [9] Burton, T., Sharpe, D., Jenkins, N., and Bossanyi, E., *Wind Energy Handbook*, John Wiley & Sons, 1st ed., 2001.

- [10] Fingersh, L. J. and Johnson, K. E., “Baseline Results and Future Plans for the NREL Controls Advanced Research Turbine Preprint,” Tech. Rep. November 2003, National Renewable Energy Laboratory, Golden, Colorado, 2003.
- [11] Vestas, *Operating Manual: Vestas V27/V29-225kW Wind Turbines for: 400V and 690V*, No. 941253, VESTAS, Aarhus, Denmark, 2nd ed., 2002.
- [12] Saylor, S. W. V. A., “Wind Power Plant Technology, Design and Operation,” 2012.
- [13] Mohan, N., *Electric drives: an integrative approach*, Minnesota Power Electronics Research & Education (MNPERE), 2003.

Appendix A

Photos of Turbine Hardware



Figure A.1: The cRIO in the tower base used for CBM.



Figure A.2: The hydraulic motor in the nacelle.

Appendix B

Physical Parameters of the V27 Wind Turbine

V27 OEM Specifications	
Rotor	
Diameter	27 m
Swept Area	573 m ²
Number of Blades	3
Blades	
Length	13 m
Width	1.3/0.5 m
Twist	13 degrees
Weight	600 kg/pcs.
Tower	
Height	30 m
Diameter Top	1.4 m
Diameter Bottom	2.4 m
Weight	12,000 kg
Heights	
Hub Height	31.5 m
Free Height	18.0 m
Highest Point	45.0 m
Operational Data	
Cut-in wind speed	3.5 m/s
Rated wind speed (225kW)	14 m/s
Cut-off wind speed	25 m/s
Gearbox	
Nominal Power	433 kW
Ratio	1 : 23.4

Table B.1: General specifications for V27 [1].